

Mahesh Kumar*

Study of differential transform technique for transient hydromagnetic Jeffrey fluid flow from a stretching sheet

<https://doi.org/10.1515/nleng-2020-0004>

Received Apr 14, 2019; accepted Nov 3, 2019.

Abstract: This article investigates the time-dependent MHD heat transfer flow of Jeffrey fluid from a stretching sheet, the topic significance to non-Newtonian viscoelastic material processing. Using similarity transformations, the governing coupled non-linear PDE's are remodel into ODE's with suitable free stream and wall boundary conditions. The developed non-dimensional non-linear problem is revealed to be analysed by several key thermophysical and rheological parameters, namely, Jeffrey fluid parameter (λ), Deborah number (β), Prandtl number (Pr), buoyancy parameter (ξ), magnetic parameter (M) and unsteadiness parameter (A). The semi-exact differential transform technique is applied to elucidate the coupled nonlinear governing equation of non-Newtonian Jeffrey fluid problem. Also, the solution is validated with numerical results attained via the MATLAB bvp4c function. Excellent accurateness is attained through the DTM approach. Further validation with available consequences from the existing literature is incorporated. The results indicate that fluid velocity and temperature are boosted with increasing Deborah number and stretching parameter however it shows a decreasing trend with Jeffrey fluid parameter and convection parameter. It also shows when augmenting the magnetic parameter which reduces the flow and increases the thickness of the boundary layer.

Keywords: DTM; Jeffrey fluid; heat transfer; stretching sheet

1 Introduction

The flow of non-Newtonian fluids with heat transfer from stretching surfaces ensures frequent engineering applications. In point, several manufacturing processes consist of

the fabrication of sheeting material which contains polymer sheets. Such kind of flows is particularly applicable in the aerodynamic extrusion of chemical compound sheets, hot rolling, petroleum reservoirs, fibers spinning, artificial fibers, continuous filament extrusion from a die, manufacturing of elastic sheet, tinning and annealing of copper wires, polymers continuous casting, and glass blowing. Originally, the revolutionary work of boundary layer flow from a stretching sheet was premeditated by Sakiadis [1] and Erickson [2]. Later, Crane [3] extended the same [1, 2] model work for 2-D flow for the stretching surface and reported the exact solution. Successively numerous investigators have further protracted the Sakiadis and Crane models for analysing suction or blowing problems [4], viscous dissipation effects [5], stagnation flows [6] and variable viscosity [7]. Conversely, in several stretching flow problems, transient behaviour ascends owing to a swift elongating of the sheet. This characterizes some cases such as flow generated by a periodic variation of the temperature or the flow over an impulsive stretching sheet. Since instantaneous developed is occur as a result of sudden stretching of the sheet with definite velocity. Interesting models related to the impulsive stretching sheet found in Ref. [8–14].

Though, the above-cited studies are circumscribed to viscous fluid (Newtonian fluids) and which are fails to explain the rheological (non-Newtonian) behaviour specifically, in polymer processing, extrusion of plastics, glass blowing, biochemical industries, coating protection, etc., The modeling studies compacts with non-Newtonian fluids offer interesting challenges to the many researchers and which specifically mimic several complex characteristics of real industrialized fluids including couple stresses, viscoelasticity, viscoplasticity, spurt, etc. In spite of various physical constitutions of non-Newtonian fluids, among all the Jeffrey fluid is one which constituents characterizing the noticeable features of retardation and relaxation times [15–19]. The application of Jeffrey fluid includes notably polymer solutions and multi-phase systems namely, emulsion, slurries, foams, etc. Also, it may consider as blood model [20–22]. Hamad et al. [23] con-

*Corresponding Author: Mahesh Kumar, Central University of Karnataka, Kalaburagi, 585367, India, E-mail: mkhmaths@gmail.com

sidered the heat transfer flow of a Jeffrey fluid problem through a stretching sheet nearby stagnation point. Turki-ilmazoglu and Pop [24] explored a similar type of problem with parallel external flow. The time-dependent flow of non-Newtonian Jeffrey fluid for stretching sheet geometry was analysed by Hayat et al. [25]. Recently, Hayat et al. [26] examined the 3-D Jeffrey fluid flow in a bidirectional stretching surface.

Magnetohydrodynamic (MHD) flow of an electrically conducting fluid as a result of the sheet geometry is of significant interest in contemporary metallurgic and metal-working processes, condensation process and also in polymer industries. It has several other applications including induction flow meter, chemical factories, in lubrication of machine components, in coolers and heaters of mechanical and electrical devices, etc. The hydromagnetic boundary layer flow of Jeffrey fluid has been premeditated by several authors [27–33]. Recently, Khan et al. [34] analysed the MHD effects of Jeffrey fluid problem from inclined stretching sheet. Qayyum et al. [35] analysed the MHD flows of Jeffrey nanofluid past a non-linear stretching surface. Zokri et al. [36] studied Jeffrey fluid with MHD effects over the sheet with the impact of dissipation. Similarly, the MHD stagnation point flow of Jeffrey fluid from a stretched surface was analysed by Hayat et al. [37].

Most of the fluid mechanics problems are basically in nonlinear form and are referred to nonlinear ordinary or partial differential equations. The analytical methods could not evaluate these types of nonlinear equations accurately. Further methods, which are numerical/semi-analytical in nature, therefore need to be employed and to handle these type of problem the authors prefer certain standard methods of decomposition technique, perturbation technique, Iteration technique, homotopy analysis and optimal asymptotic techniques and similarly, differential transform technique. These semi-analytical/numerical methods are recurrently applied on account of their greater exactness and ease in producing results. In the current article, the Differential Transform Method (DTM) [38] is hired. It is a vigorous semi-exact method, which is not constructed on the subsistence of large or small factors. This method has essential benefits over the other estimated semi-exact methods. It is useful to solve various differential equations viz. difference equation, eigenvalue problems, nonlinear integral, high index, differential-algebraic equations fractional, pantograph equation, nonlinear oscillators and integro-differential equation without restrictive assumptions, linearization, perturbation, discretization or round-off error. Many researchers applied DTM to solve various flow-field problems. Hatami et al. [39] applied the DTM to

solve the non-Newtonian fluid flow problem for plate geometry. Recently, Sobamowo [40] applied DTM to analyse the 2D nanofluid problem from the porous channel. Usman et al. [41] studied the DTM to examine the transient nanofluid flow problem. Other recent work on DTM can be found in ref. [42–44]. A close review of the earlier literature survey specifies that a very less number of analysis have been done for the DTM study on nonlinear transient flow of Jeffrey fluid over a sheet. Therefore, the existing study aspires to discuss the DTM to the convective heat transfer flow of Jeffrey fluid over a stretching sheet problem.

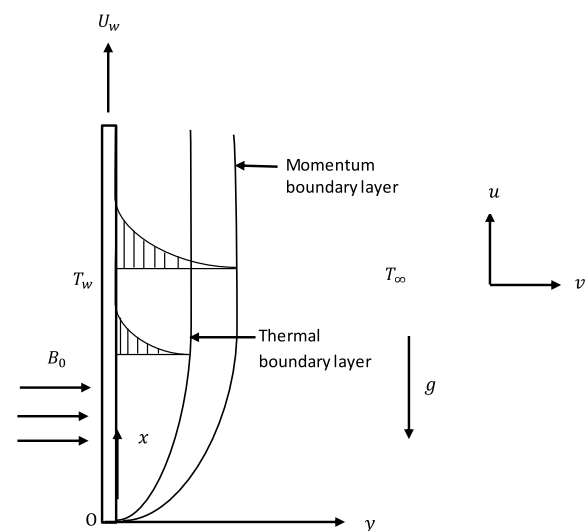


Figure 1: Geometry of the present investigated problem

2 Mathematical modelling

Transient, 2-D, incompressible, laminar thermal convective electrically conducting Jeffrey fluid flow over stretching sheet geometry is deliberated and is described in Figure 1. In the beginning i.e., $t = 0$, the considered sheet is precipitately stretched by velocity $U_w(x, t)$ along the direction of x -axis, by fixing origin with ambient fluid temperature T_∞ and sheet temperature $T_w(x, t)$ is presumed to vary linearly from the x -coordinate. The stationary Cartesian coordinate system has its fixed origin placed at the forefront of the sheet in which x -axis is taken alongside the sheet in an upward direction and the y -axis positioned normal direction to the sheet. Following by all these suppositions (with the approximations of Boussinesq and boundary layer), the mathematical governing non-linear equations for hydromagnetic flow of Jeffrey fluid with heat

transfer [25, 26] are:

$$\frac{\partial u}{\partial x} + \frac{\partial v}{\partial y} = 0 \quad (1)$$

$$\begin{aligned} \frac{\partial u}{\partial t} + u \frac{\partial u}{\partial x} + v \frac{\partial u}{\partial y} &= g\beta_T (T - T_\infty) \\ &+ \frac{g}{1+\lambda} \left[\frac{\partial^2 u}{\partial y^2} + \lambda_1 \left(\frac{\partial^3 u}{\partial y^2 \partial t} + v \frac{\partial^3 u}{\partial y^3} + \frac{\partial u}{\partial y} \frac{\partial^2 u}{\partial x \partial y} \right. \right. \\ &\left. \left. + u \frac{\partial^3 u}{\partial x \partial y^2} - \frac{\partial u}{\partial x} \frac{\partial^2 u}{\partial y^2} \right) \right] - \frac{\sigma B_0^2 u}{\rho} \end{aligned} \quad (2)$$

$$\frac{\partial T}{\partial t} + u \frac{\partial T}{\partial x} + v \frac{\partial T}{\partial y} = \alpha \frac{\partial^2 T}{\partial y^2} \quad (3)$$

The appropriate boundary conditions on the flow are given by:

$$T = T_w, \quad v = 0, \quad u = U_w \text{ at } y = 0$$

$$T \rightarrow T_\infty, \quad u \rightarrow 0, \quad \frac{\partial u}{\partial y} \rightarrow 0 \text{ as } y \rightarrow \infty \quad (4)$$

The assumptions of sheet velocity and temperature namely, $U_w(x, t)$ and $T_w(x, t)$ are given by

$$U_w(x, t) = \frac{ax}{(1-ct)}$$

and

$$T_w(x, t) = T_\infty + \frac{bx}{(1-ct)^2}, \quad (5)$$

Where the constants a and c (with $a > 0$ and $c \leq 0$, where $ct < 1$) are measured in terms of frequency units i.e. $(\text{time})^{-1}$, while the constant b is measured in unit of temperature/length, with $b < 0$ and $b > 0$ relate to the buoyancy opposing flow and buoyancy assisting flow, respectively. Furthermore $b = 0$ corresponds to forced convection flow. It is noteworthy that at the outset, i.e. $t = 0$, the governing system of Eqs. (1)-(3) reduces to the steady flow situation. These specific forms of $U_w(x, t)$ and $T_w(x, t)$ have been desired so as to extract a novel similarity variables, which modifies the governing non-linear PDE's (Eqs. (1) - (3)) into a set of ODE's. Succeeding with the scrutiny, let us consider the subsequent non-dimensional functions f and θ , and similarity variable η as follows [8, 9]:

$$\eta = \sqrt{\frac{a}{v(1-ct)}} y, \quad \psi = \sqrt{\frac{av}{(1-ct)}} x f(\eta), \quad \theta(\eta) = \frac{T - T_\infty}{T_w - T_\infty}, \quad (6)$$

Here $\psi(x, y, t)$ denotes stream function and is well-defined in standard way as $(u, v) = \left(\frac{\partial \psi}{\partial y}, -\frac{\partial \psi}{\partial x} \right)$ which satisfies the equation (1) in the exact manner. Now, Substituting Eqn. (6) into (2) and (3) we get:

$$f'''' + (1+\lambda) \left(f'' - f'^2 - A \left(\frac{1}{2} \eta f'' + f' \right) + \xi \theta - M f' \right)$$

$$+ \beta \left(2ff'' - f''^2 - f' f'''' + A \left(\frac{1}{2} \eta f'''' + 2f'' \right) \right) = 0 \quad (7)$$

$$\frac{1}{Pr} \theta'' + f\theta' - \theta f' - A \left(\frac{1}{2} \eta \theta' + 2\theta \right) = 0. \quad (8)$$

Here prime represents differentiation pertaining to η , $\beta = a\lambda_1/v^2\rho(1-ct)$ is the Deborah number, λ denotes the Jeffrey fluid parameter, $A = c/a$ is the stretching ratio parameter. Also, ξ is the buoyancy parameter which is defined as $\xi = Gr/Re^2$ where $Gr = g\beta_T(T_w - T_\infty)x^3/v^2$ signifies local Grashof number, $Pr = \nu/\alpha$ is the Prandtl number and $Re = U_w x/\nu$ represents the local Reynolds number. Further, ξ is non-dimensional constant with $\xi < 0$ implies buoyancy opposing flow and $\xi > 0$ related buoyancy assisting flow respectively, $\xi = 0$ signifies the forced convection flow. The associate boundary conditions are:

$$f(0) = 0, \quad f'(0) = 1, \quad \theta(0) = 1 \text{ at } \eta = 0$$

$$f'(\eta) \rightarrow 0, \quad f''(\eta) \rightarrow 0, \quad \theta(\eta) \rightarrow 0 \text{ as } \eta \rightarrow \infty \quad (9)$$

The essential physical parameters of wall gradient features such as friction C_f , shear stress at the sheet surface τ_w , heat transfer rate Nu and surface heat flux q_w are well-defined as follows:

$$C_f = \frac{\tau_w}{\rho U_w^2/2},$$

$$\tau_w = -\frac{\mu}{1+\lambda} \left[\frac{\partial u}{\partial y} + \lambda_1 \left(u \frac{\partial^2 u}{\partial x \partial y} + v \frac{\partial^2 u}{\partial y^2} \right) \right]_{y=0}$$

then

$$\frac{1}{2} (1+\lambda) C_f Re^{1/2} = \left[f''(0) + \beta \left\{ f'(0) f''(0) - f(0) f'''(0) \right\} \right] \quad (10a)$$

$$Nu = \frac{q_w}{T_w - T_\infty} \left(\frac{x}{k} \right), \quad q_w = -k \left(\frac{\partial T}{\partial y} \right)_{y=0}$$

$$\text{then } Nu/Re^{1/2} = -\theta'(0) \quad (10b)$$

3 Differential transform method solutions

The nonlinear dimensionless well-defined ordinary differential Eqs. (7) – (9) of the boundary value problem is elucidated with DTM. Zhou proposed the idea of DTM for the first time in 1986 [38] and it was developed to evaluate the non-linear and linear forms of IVP's in the analysis of

the electric circuit. This DTM composes an analytical result in the polynomial form and it is completely based on the standard Taylor-series method. The foremost advantage of DTM is used for elucidating nonlinear mathematical equations without necessitating linearization, and discretization. Hence, the method does not pretend by errors related to discretization. It also eases the size of the computational part and it is pertinent to numerous mathematical problems easily. DTM has been implemented successfully in several fluid dynamics, multi-physical mechanics, and heat transfer models in the current centuries. These include Burgers and coupled Burgers equations [45], application to nonlinear oscillators [46], plane Couette fluid flow problem [47], free vibration analysis [48], micropolar fluid flows [49, 50], non-Newtonian nanofluids flow analysis [51], solving nonlinear dynamic problems [52], Acoustic and Wave propagation problems [53] and viscoelastic Winkler foundation [54]. Differential Transform Method has been revealed to be a very effective way in this article. Though convergence can be hastened with alterations of this method e.g. Padé estimations, it is not compulsory. The complete procedure of the method to the present problem is now defined. The k th derivative of differential transform of the function $f(\eta)$ is well-defined as:

$$F(p) = \frac{1}{p!} \left[\frac{d^p f(\eta)}{d\eta^p} \right]_{\eta=\eta_0} \quad (11)$$

where $f(\eta)$ represents original function and $F(p)$ signifies transformed function. The inverse differential transformation is as follows:

$$f(\eta) = \sum_{p=0}^{\infty} F(p)(\eta - \eta_0)^p, \quad (12)$$

For the practical models, the function $f(\eta)$ is expressed by a truncated series and hence the above Eqn. (12) can be written as:

$$f(\eta) = \sum_{p=0}^m F(p)(\eta - \eta_0)^p. \quad (13)$$

Eqn. (13) implies that $\sum_{p=m+1}^{\infty} F(p)(\eta - \eta_0)^p$ is trivially small, where m denotes the series size in this problem. Few essential of the assets of DTM are revealed in Table 1. These assets are obtained from Eqs. (12) and (13).

Now, implementing DTM and taking differential transform of non-linear governing conservation Eqs. (7) and (8) along with corresponding boundary conditions (9) we get subsequent recurrence relations as follow:

$$(p+1)(p+2)(p+3)F(p+3) + (1+\lambda_1) \sum_{r=0}^p (F[p-r](p+1)(p+2)F(p+2))$$

$$\begin{aligned} & - (1+\lambda) \sum_{r=0}^p ((p-r+1)F[p-r+1](p+1)F(p+1)) \\ & - (1+\lambda) A \left(\frac{1}{2} \sum_{r=0}^p (\delta(p-r+1)(p+1)(p+2)F(p+2)) \right. \\ & \quad \left. + (p+1)F(p+1) \right) + (1+\lambda) \xi G[p] \\ & - (1+\lambda) M(p+1)F[p+1] \\ & + 2\beta \sum_{r=0}^p (F[p-r](p+1)(p+2)(p+3)F(p+3)) \\ & - \beta \sum_{r=0}^p ((p-r+1)(p-r+2)F[p-r+2] \\ & \quad (p+1)(p+2)F(p+2)) \\ & + \beta \sum_{r=0}^p ((p-r+1)F[p-r+1] \\ & \quad (p+1)(p+2)(p+3)(p+4)F(p+4)) \\ & + \beta A \left(\frac{1}{2} \sum_{r=0}^p (\delta(p-r+1)(p+1)(p+2)(p+3)(p+4)F \right. \\ & \quad \left. (p+4)) + 2(p+1)(p+2)(p+3)F(p+3) \right) = 0 \quad (14) \end{aligned}$$

$$\begin{aligned} & \frac{1}{Pr} (p+1)(p+2)G(p+2) \\ & - A \left(\frac{1}{2} \sum_{r=0}^p (\delta(p-r+1)(p+1)G(p+2)) + 2G(p) \right) \\ & + \sum_{r=0}^p (F[p-r+1](p+1)G(p+1)) \\ & - \sum_{r=0}^p (G[p-r+1](p+1)F(p+1)) = 0 \quad (15) \end{aligned}$$

Corresponding boundary conditions:

$$F[0] = 0, F[1] = 1, F[2] = \frac{n_1}{2}, F[3] = \frac{n_2}{6}, \quad (16a)$$

$$G[0] = 0, G[1] = n_3 \quad (16b)$$

where $F(p)$, $G[p]$ are the differential transform of $f(\eta)$, $\theta(\eta)$ and n_1, n_2, n_3 are unknowns which can be calculated from boundary conditions i.e. Eqn. (9).

Following relations can be obtained through transformed boundary conditions (16a) and (16b):

$$\begin{aligned} F[4] &= (-1 + n_2 + n_1^2 \beta - n_2 \beta + (2An_2)\beta - \lambda \\ & - A(1+\lambda)\xi(1+\lambda) - M(1+\lambda))/24\beta \quad (17a) \end{aligned}$$

$$\begin{aligned} F[5] &= (2n_1 n_2 \beta - n_1(1+\lambda) - Mn_1(1+\lambda) - (An_1)(1+\lambda) \\ & + \xi n_3(1+\lambda) + (-1 + n_2 + n_1^2 \beta - n_2 \beta + (2An_2)\beta - \lambda \end{aligned}$$

Table 1: Fundamental basic operations of DTM [38]

Original function	Transformed function
$f(\eta) = g(\eta) \pm h(\eta)$	$F(p) = G(p) \pm H(p)$
$f(\eta) = cg(\eta)$	$F(p) = cG(p)$
$f(\eta) = \frac{d^n g(\eta)}{d\eta^n}$	$F(p) = \frac{(p+n)!}{p!} G(p+n)$
$f(\eta) = g(\eta)h(\eta)$	$F(p) = \sum_{r=0}^p G(r)H(p-r)$
$f(\eta) = \eta^n$	$F(p) = \delta(p-n) = \begin{cases} 1, & \text{if } p = n \\ 0, & \text{if } p \neq n \end{cases}$

$$\begin{aligned}
& -(1+\lambda)A + (1+\lambda)\xi - M(1+\lambda))/\beta \\
& -\beta(n_1n_2 + (-1+n_2+n_1^2\beta - n_2\beta + (2An_2)\beta \\
& -\lambda - (1+\lambda)A + (1+\lambda)\xi - M(1+\lambda))/\beta \\
& -\beta(2A(-1+n_2+n_1^2\beta - n_2\beta + (2An_2)\beta - \lambda - (1+\lambda)A \\
& + (1+\lambda)\xi - M(1+\lambda))/\beta)/120\beta \quad (17b)
\end{aligned}$$

$$\begin{aligned}
F[6] &= \left(-\frac{1}{2}Mn_2(1+\lambda) + \left(\frac{n_1^2}{2} + n_2\right)(1+\lambda) - (n_1^2 + n_2)(1+\lambda) + A\frac{n_2}{2}(1+\lambda) + \frac{1}{2}(1+2A)\xi \Pr(1+\lambda) \right. \\
& + \beta(n_2^2 + \frac{1}{\beta}(-1+n_2+n_1^2\beta - n_2\beta \\
& + (2An_2)\beta + (1+\lambda)\xi - A(1+\lambda) - \lambda - (1+\lambda)M)) \\
& + (2n_1n_2\beta - n_1(1+\lambda) - Mn_1(1+\lambda) - (An_1)(1+\lambda) \\
& + \xi n_3(1+\lambda) + (-1+n_2+n_1^2\beta - n_2\beta + (2An_2)\beta - \lambda \\
& - (1+\lambda)A + (1+\lambda)\xi - M(1+\lambda))/\beta \\
& -\beta(n_1n_2 + (-1+n_2+n_1^2\beta - n_2\beta + (2An_2)\beta - \lambda \\
& - (1+\lambda)A + (1+\lambda)\xi - M(1+\lambda))/\beta) \\
& -\beta(2A(-1+n_2+n_1^2\beta - n_2\beta + (2An_2)\beta - \lambda \\
& - (1+\lambda)A + (1+\lambda)\xi - M(1+\lambda))/\beta)/2\beta \\
& + \beta\left(\frac{n_2^2}{2} + \frac{n_1}{\beta}(-1+n_2+n_1^2\beta - n_2\beta + (2An_2)\beta - \lambda \right. \\
& - A(1+\lambda) + \xi(1+\lambda) - (1+\lambda)M) \\
& + (2n_1n_2\beta - n_1(1+\lambda) - Mn_1(1+\lambda) - (An_1)(1+\lambda) \\
& + \xi n_3(1+\lambda) + (-1+n_2+n_1^2\beta - n_2\beta + (2An_2)\beta - \lambda \\
& - (1+\lambda)A + (1+\lambda)\xi - M(1+\lambda))/\beta \\
& -\beta(n_1n_2 + (-1+n_2+n_1^2\beta - n_2\beta + (2An_2)\beta - \lambda \\
& - (1+\lambda)A + (1+\lambda)\xi - M(1+\lambda))/\beta) \\
& -\beta(2A(-1+n_2+n_1^2\beta - n_2\beta + (2An_2)\beta - \lambda \\
& - (1+\lambda)A + (1+\lambda)\xi - M(1+\lambda))/\beta)/2\beta
\end{aligned}$$

$$\begin{aligned}
& + A(-1+n_2+n_1^2\beta - n_2\beta + (2An_2)\beta - \lambda \\
& - A(1+\lambda) + \xi(1+\lambda))/\beta - M(1+\lambda) \\
& + (2n_1n_2\beta - n_1(1+\lambda) - Mn_1(1+\lambda) - (An_1)(1+\lambda) \\
& + \xi n_3(1+\lambda) + (-1+n_2+n_1^2\beta - n_2\beta + (2An_2)\beta \\
& + \xi(1+\lambda) - \lambda - A(1+\lambda) - M(1+\lambda))/\beta \\
& -\beta(n_1n_2 + (-1+n_2+n_1^2\beta - n_2\beta + (2An_2)\beta + \xi(1+\lambda) \\
& - \lambda - A(1+\lambda) - M(1+\lambda))/\beta) \\
& -\beta(2A(-1+n_2+n_1^2\beta - n_2\beta + (2An_2)\beta - \lambda - A(1+\lambda) \\
& + \xi(1+\lambda) - M(1+\lambda))/\beta)/2\beta)/360\beta \quad (17c)
\end{aligned}$$

$$G[2] = \frac{Pr}{2}(1+2A), \quad (18a)$$

$$G[3] = \frac{Pr}{6}(n_1 + 2An_3), \quad (18b)$$

$$\begin{aligned}
G[4] &= \frac{Pr n_1 n_3}{24} + \frac{Pr n_2}{24} - \frac{1}{24}Pr^2(1+2A) \\
& + \frac{1}{12}Pr^2 A(1+2A), \quad (18c)
\end{aligned}$$

$$\begin{aligned}
G[5] &= \frac{Pr n_2 n_3}{60} - \frac{1}{60}Pr^2(n_1 + 2An_3) \\
& + \frac{1}{60}Pr^2 A(n_1 + 2An_3) + Pr(-1+n_2+n_1^2\beta - n_2\beta \\
& + (2An_2)\beta - \lambda - A(1+\lambda) + \xi(1+\lambda) - M(1+\lambda))/120\beta, \quad (18d)
\end{aligned}$$

$$\begin{aligned}
G[6] &= \frac{1}{12}Pr n_2(1+2A) - \frac{1}{12}Pr n_1(n_1 + 2An_3) \\
& - \frac{Pr n_1 n_3}{8} + \frac{Pr n_2}{8} - \frac{1}{8}Pr^2(1+2A) \\
& + \frac{1}{12}Pr^2 A(1+2A) + \dots \quad (18e)
\end{aligned}$$

The above solution procedure is goes on. By substituting Eqs. (17) and (18) in Eqn. (13) based on DTM, the series solutions can be formed as:

$$f(\eta) = \eta + \frac{n_1 \eta^2}{2} + \frac{n_2 \eta^3}{6} + \left((-1 + n_2 + n_1^2 \beta - n_2 \beta + (2A n_2) \beta - \lambda - A(1 + \lambda) \xi(1 + \lambda) - M(1 + \lambda)) \eta^4 \right) / (24\beta) + \dots \quad (19)$$

$$\theta(\eta) = 1 + n_3 \eta + \frac{1}{2} Pr(1 + A) \eta^2 + \frac{1}{6} Pr(n_1 + 2A n_3) \eta^3 + \left(\frac{Pr n_1 n_3}{24} + \frac{Pr n_2}{24} - \frac{1}{24} Pr^2 (1 + 2A) + \frac{1}{12} Pr^2 A (1 + 2A) \right) \eta^4 + \dots \quad (20)$$

From the above Eqs. (19) and (20) the unidentified n_1, n_2, n_3 values are evaluated by using boundary conditions stated in eqn. (9). Afterwards, substituting the n_1, n_2, n_3 into the Eqs. (19) and (20) for selected case of control parameters ($\xi = 1.0, \lambda = 0.2, A = 0.2, Pr = 1.0, \beta = 0.2, M = 1.0$), the expressions of $f(\eta)$ and $\theta(\eta)$ can be written as follows:

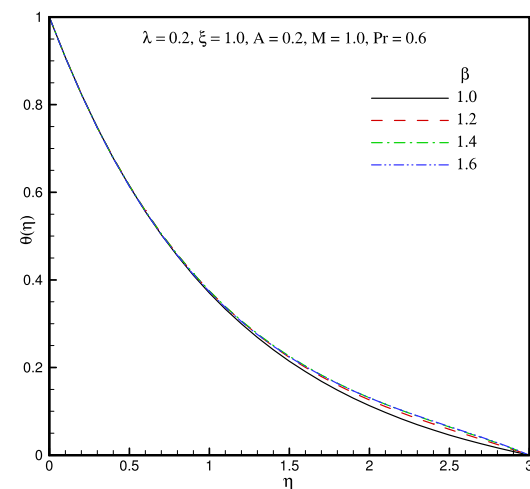
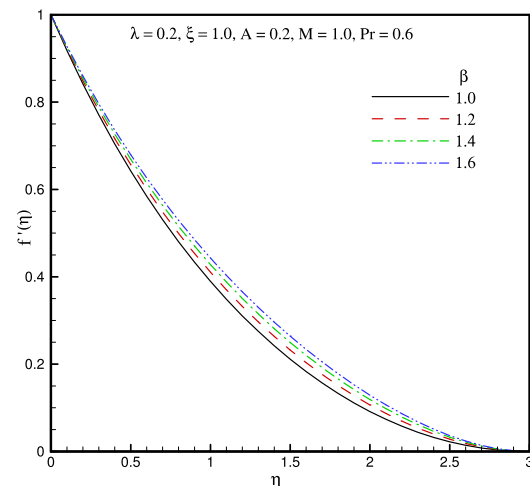
$$f(\eta) = \eta - 0.5694084829591259 \eta^2 + 0.1787519035193708 \eta^3 - 0.049335236051056504 \eta^4 + 0.01041152884895365 \eta^5 + 0.0006332482535334163 \eta^6 + \dots \quad (21)$$

$$\theta(\eta) = 1 - 1.2253008931244445 \eta + 0.7 \eta^2 - 0.2714895538613383 \eta^3 + 0.06782936944004704 \eta^4 - 0.010050369604302202 \eta^5 + 0.0009196895849455119 \eta^6 \quad (22)$$

In order to corroborate the present existing results of the considered problem and endorse accuracy, the obtained DTM results are equated with existing available numerical results as described in Table 2 for various values of physical parameter, from which one can see that results of DTM computations are in good agreement. The numerical result of the present model is performed with the help of MATLAB built in solver. Additionally, the current DTM results are also compared in Table 3 with those obtainable results for the case of Newtonian fluid ($\beta = 0, \lambda = 0, M = 0$) of Ishak et al. [7] for absence of the buoyancy term $\xi \theta$ in Eqn. (7) and $Pr = 1.0$ and $A = 0$ (steady-state flow). Yet again, an excellent correspondence is achieved which endorses the validity of the DTM computations.

4 Results and discussion

With the aim of analyse physical insight of the considered model the graphical results of the flow-field profiles have been discussed for several values of control parameters such as Deborah number β , Jeffrey fluid parameter λ , unsteadiness parameter A , convection parameter ξ and Prandtl number Pr . The simulated results are computed and are presented graphically in Figures 2-6.



(b)

Figure 2: Simulated velocity and temperature profiles for various values of Deborah number

The consequences of Deborah number β on velocity $f'(\eta)$ and temperature $\theta(\eta)$ profile are presented in Figures 2a and 2b. As β increases, the velocity and the boundary layer thickness is increases. This is due to the existence

Table 2: Variation of skin-friction coefficient ($-\frac{1}{2}C_f Re^{1/2}$) for different physical parameter values

A	Pr	ξ	λ	β	Present	CPU	Numerical	CPU	Error
0.1	0.6	1.0	0.2	1.0	2.4981	18.5464	2.4958	992.8594	0.0007
0.2					2.7769	18.9718	2.7778	903.0781	0.0009
0.2	0.8				2.3307	17.4375	2.3315	1000.0694	0.0008
	0.6	0.3			1.9092	18.3947	1.9097	1000.0906	0.0005
		0.5			2.0951	18.7325	2.0955	1000.1177	0.0004
		1.0	0.4		3.4952	17.9865	3.4957	1000.2980	0.0005
			0.2	1.2	2.2385	16.6405	2.2386	1000.3934	0.0001
				1.4	2.7766	16.9562	2.7768	1000.4176	0.0002

Table 3: Values of $-\theta'(0)$ for $\beta = 0$, $M = 0$, $\lambda = 0$

A	ξ	Ishak <i>et al.</i> [7]	Numerical results	Present results
0	0	1.0000	1.0581	1.0749
	1	1.0873	1.1090	1.1162
	2	1.1423	1.1514	1.1609
	3	1.1853	1.1880	1.2039
1	0	1.6820	1.6860	1.7066
	1	1.7029	1.7058	1.7286

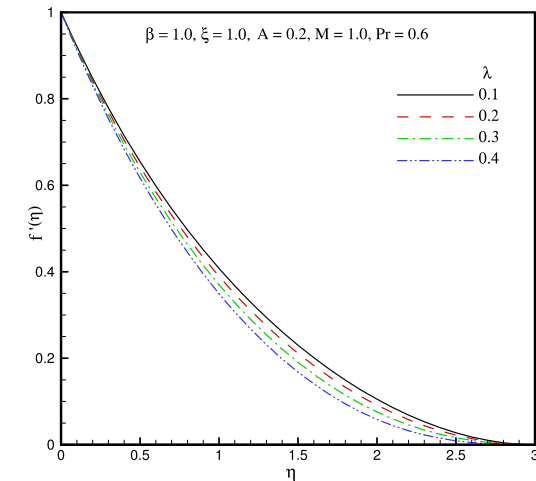
of rheological features of viscoelastic flow and impermeability of the wall upsurge the flow velocity and thickness of the boundary layer. It has also been remarked that the influence of β is to augment the temperature and thermal boundary layer thickness become lesser.

Figures 3a-3b portray the influence of λ on velocity and temperature curves through the boundary layer. From Figure 3a, the velocity declines for augmenting values of λ with the augmenting distance (η) of the sheet. Physically as λ being the viscoelastic parameter displays it shows

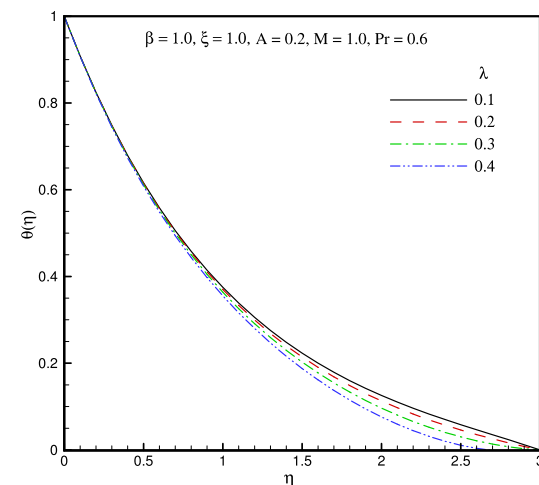
both elastic and viscous characteristics or more we can say it augments non-Newtonian behaviour and as a consequence it boosts boundary layer thickness. Therefore, the fluid motion is slow down and velocity reduces. The temperature profile in Figure 3b shows the similar trend as that of velocity. As λ become higher, the temperature decreases negatively along the sheet.

The impact of unsteadiness parameter A on velocity and temperature distribution is demonstrated in Figures 4a and 4b, respectively. Scrutiny of Figure 4a reveals that velocity shows a increasing tendency with amplified values of A . Since A is reciprocal of positive constant coefficient α . Thus, boost in the A values upturns the stretching ratio. This results the increment in velocity. Also, the temperature profile displays analogous trend for variation of A values when $0 < \eta < 1.2$. Conversely, the reverse trend is exhibited for $\eta > 1.2$ as illustrated in Figure 4b.

Figures 5a and 5b respectively elucidate the effect of convection parameter ξ on flow field profiles. The variation of cumulative values of ξ is to decrease the velocity. Substantially $\xi > 0$ signifies assisting flow, $\xi < 0$ reveals opposing flow and $\xi = 0$ implies forced convection flow. It is examined that flow velocity is reduces increasing ξ values. Since greater values of ξ relates to the extreme buoyancy pressure force greater than viscous force and which

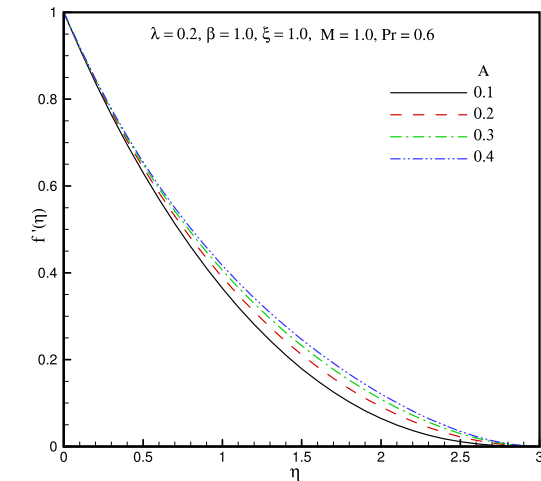


(a)

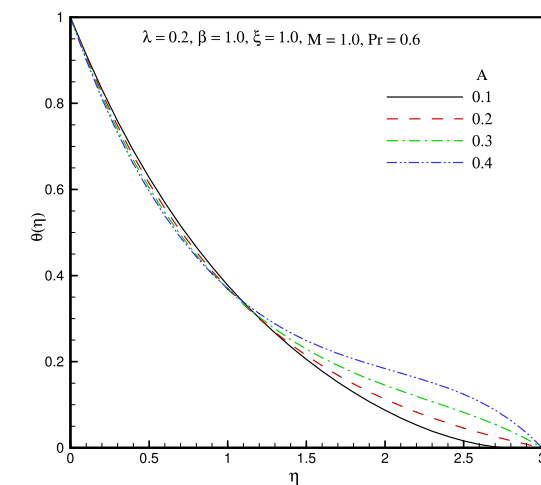


(b)

Figure 3: Simulated velocity and temperature profiles for different values of Jeffrey fluid parameter



(a)



(b)

Figure 4: Simulated velocity and temperature profiles for different values of unsteadiness parameter

results in the decrease in fluid velocity. Also, boosting values of ξ yields a marked decrease in temperatures of the fluid at the surface regime considerably and the thickness of the thermal boundary layer becomes trim down.

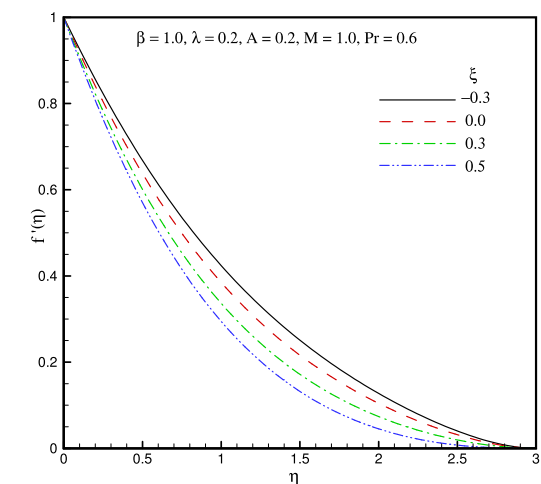
Figures 6a and 6b represent the influence of Pr on simulated flow-field profiles. Figure 6a reveals that with higher Pr values (thermal conductivity reduces) the fluid flow is slow down, and the momentum boundary layer thickness is decreased. Correspondingly, the temperature profiles are lessened with augmenting Pr values as perceived in Figure 6b. Also, the temperature variation is much more important for lower values of Pr when compared with greater values. Fluid with lower values of Pr (< 1) signify liquid-like components, which possess higher thermal conductivities but low viscosity. On the other

hand, high-viscosity oils are characterized by large values of Pr (> 1).

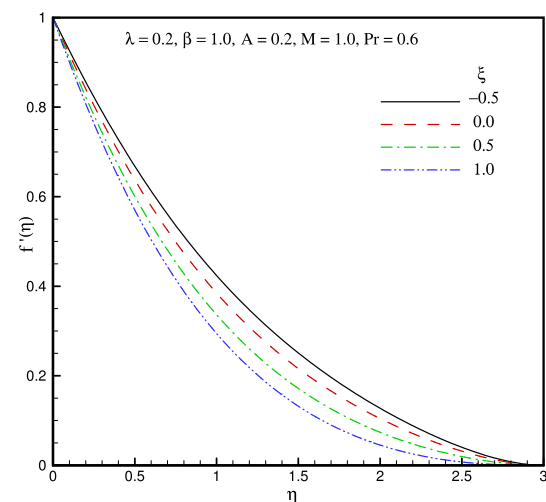
Finally, Figures 7a and 7b display the variation of MHD parameter M on distribution of velocity and temperature curves. The velocity and temperature decreasing with increase M values. The applied magnetic field develops the resistive force so-called Lorentz force. Due to this fluid movement tend to decelerate, which results to the reduction in velocity and temperature boundary layer.

5 Conclusions

In this work, a semi-analytical approach of differential transform method for resolving nonlinear coupled govern-



(a)

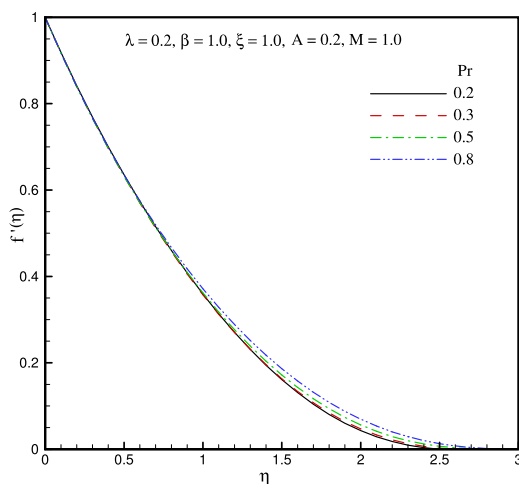


(b)

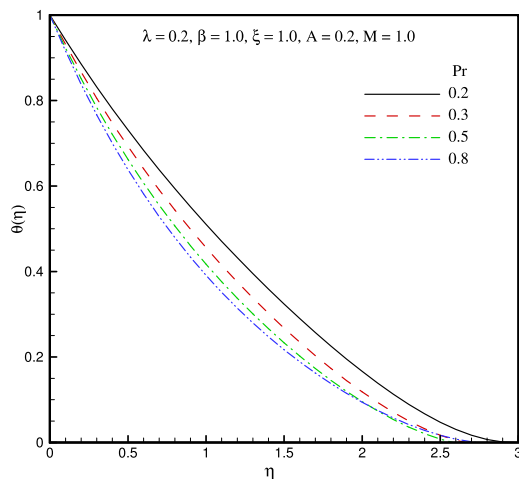
Figure 5: Simulated velocity and temperature graphs for various values of convection parameter

ing equations is presented to reveal the validity and ease of this method. For elucidating the correctness of described method, a numerical method via the **MATLAB** symbolic code 'bvp4c' was also used to solve the problems. Further comparison of present solutions with available existing literature is incorporated. The present calculations reveal that:

- The flow is boosted with increasing Deborah number whereas it is slow down with Jeffrey fluid parameter.
- Temperature is augments with Deborah number while it is depleted with Jeffrey fluid parameter.
- Increasing stretching parameter, the velocity increases and temperature reduces.



(a)



(b)

Figure 6: Simulated velocity and temperature profiles for various values of Prandtl number

- Temperature and thickness of the thermal boundary layer are reduced with increasing values of convection parameter.
- Velocity and temperature profiles opposite sign of each other for increasing values of Prandtl number.
- Increasing values of magnetic parameter, the flow-field variables show the decreasing trend.
- Excellent accurateness is attained via DTM method which holds major potential for multi-physical fluid dynamics modelling.

Acknowledgements: The authors wish to express their gratitude to the reviewers who highlighted important areas for improvement in this article. Their suggestions have served to enhance the clarity and depth of the interpretation in particular.

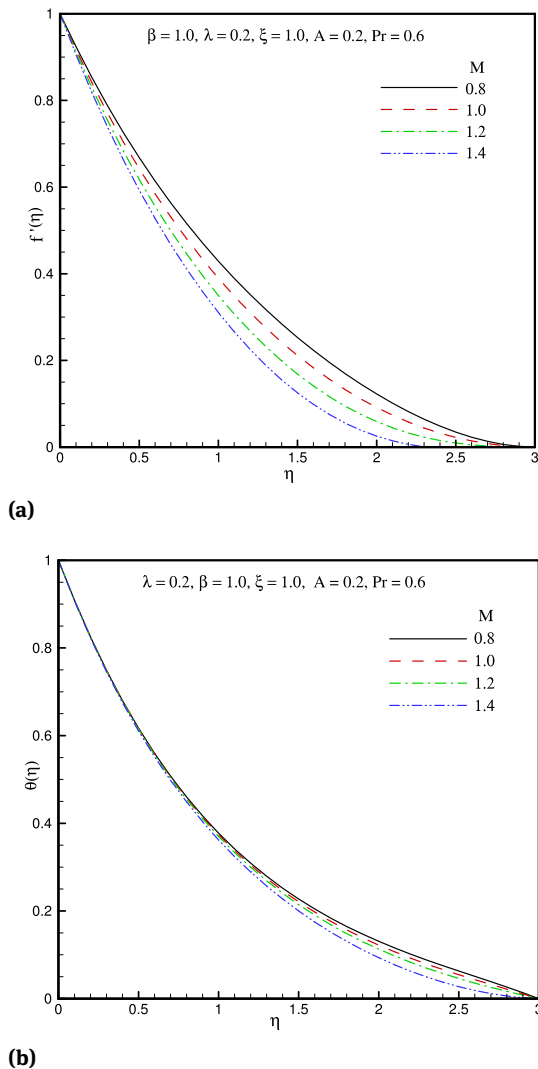


Figure 7: Simulated velocity and temperature profiles for various values of magnetic parameter

References

- [1] Sakiadis B.C., Boundary-layer behaviour on continuous solid surfaces I: The boundary-layer on an equation for two dimensional and axisymmetric flow, *AIChEJ*, 1961, 7, 26-28.
- [2] Erickson L.E., Fan L.T., Fox V.G., Heat and mass transfer on a moving continuous flat plate with suction or injection, *Ind. Eng. Chem. Fund.*, 1966, 5, 19-25.
- [3] Crane L.J., Flow past a stretching plate, *J. Appl. Math Phys.*, 1970, 21, 645-647.
- [4] Gupta P.S., Gupta A.S., Heat and mass transfer on a stretching sheet with suction or blowing, *The Can. J. Chem. Eng.*, 1977, 55, 744-746.
- [5] Alinejad J., Samarbakhsh S., Viscous flow over nonlinearly stretching sheet with effects of viscous dissipation, *J. Appl. Math.*, 2012, 2012, 1-10.
- [6] Boutros Y.Z., Abd-el-Malek M.B., Badran N.A., Hassan H.S., Lie-group method of solution for steady two-dimensional boundary-layer stagnation-point flow towards a heated stretching sheet placed in a porous medium, *Meccanica*, 2006, 41, 681-691.
- [7] Mukhopadhyay S., Layek G.C., Effects of variable fluid viscosity on flow past a heated stretching sheet embedded in a porous medium in presence of heat source/sink, *Meccanica*, 2012, 47, 863-876.
- [8] Ishak A., Nazar R., Pop I., Boundary layer flow and heat transfer over an unsteady stretching vertical surface, *Meccanica*, 2009, 44, 369-375.
- [9] Andersson H.I., Aarseth J.B., Dandapat B.S., Heat transfer in a liquid film on an unsteady stretching surface, *Int. J. Heat Mass Transf.*, 2000, 43, 69-74.
- [10] Na T.Y., Pop I., Unsteady flow past a stretching sheet, *Mech. Res. Commun.*, 1996, 23, 413-422.
- [11] Wang C.Y., Du G., Miklavi M., Chang C.C., Impulsive stretching of a surface in a viscous fluid, *SIAM J. Appl. Math.*, 1997, 57, 1-14.
- [12] Elbashbeshy E.M.A., Bazid M.A.A., Heat transfer over an unsteady stretching surface, *Heat Mass Transf.*, 2004, 41, 1-4.
- [13] Nazar R., Amin N., Filip D., Pop I., Unsteady boundary layer flow in the region of the stagnation point on the stretching sheet, *Int. J. Eng. Sci.*, 2004, 42, 1241-1253.
- [14] Devi C.D.S., Takhar H.S., Nath G., Unsteady mixed convection flow in stagnation region adjacent to a vertical surface, *Heat and Mass Trans.*, 1991, 26, 71-79.
- [15] Hayat T., Waqas M., Shehzad S.A., Alsaedi A., MHD stagnation point flow of Jeffrey fluid by a radially stretching surface with viscous dissipation and Joule heating, *J. Hyd. Hydromech.*, 2015, 63, 311-317.
- [16] Hayat T., Mustafa M., Influence of thermal radiation on the unsteady mixed convection flow of a Jeffrey fluid over a stretching sheet, *Zeitschrift für Naturf.*, 2010, 65a, 711-719.
- [17] Abbasi F.M., Shehzad S.A., Hayat T., Alsaedi A., Obid M.A., Influence of heat and mass flux conditions in hydromagnetic flow of Jeffrey nanofluid, *AIP Adv.*, 2015, 5, 037111.
- [18] Farooq M., Alsaedi A., Hayat T., Note on characteristics of homogeneous- heterogeneous reaction in flow of Jeffrey fluid, *Appl. Math. Mech.*, 2015, 36, 1319-1328.
- [19] Tripathi D., Ali N., Hayat T., Chaube M.K., Hendi A.A., Peristaltic flow of MHD Jeffrey fluid through a finite length cylindrical tube, *Appl. Math. Mech. (Eng. Ed.)*, 2011, 32, 1148-1160.
- [20] Nadeem S., Akbar N.S., Peristaltic flow of a Jeffrey fluid with a variable viscosity in an asymmetric channel, *Zeitschrift Naturf. A.*, 2009, 64a, 713-722.
- [21] Srinivas S., Muthuraj R., Peristaltic transport of a Jeffrey fluid under the effect of slip in an inclined asymmetric channel, *Int. J. Appl. Mech.*, 2010, 02, 437-455.
- [22] Vajravelu K., Sreenadh S., Devaki P., Prasad K.V., Peristaltic transport of a Herschel-Bulkley fluid in an elastic tube, *Heat Transf. Asian Res.*, 2015, 44, 585-598.
- [23] Hamad M.A.A., AbdEl-Gaied S.M., Khan W.A., Thermal jump effects on boundary layer flow of a Jeffrey fluid near the stagnation point on a stretching/shrinking sheet with variable thermal conductivity, *J. Fluids*, 2013, 2013, 1-9.
- [24] Turkyilmazoglu M., Pop I., Exact analytical solutions for the flow and heat transfer near the stagnation point on a stretching/shrinking sheet in a Jeffrey fluid, *Int. J. Heat and Mass Trans.*, 2013, 57, 82-88.

- [25] Hayat T., Iqbal Z., Mustafa M., Alsaedi A., Unsteady flow and heat transfer of Jeffrey fluid over a stretching sheet, *Thermal Sci.*, 2014, 18, 1069-1078.
- [26] Hayat T., Asad S., Mustafa M., Alsaedi A., MHD stagnation-point flow of Jeffrey fluid over a convectively heated stretching sheet, *Comp. Fluids*, 2015, 108, 179-185.
- [27] Shehzad S.A., Hayat T., Alsaedi A., Obid M.A., Nonlinear thermal radiation in three-dimensional flow of Jeffrey nanofluid: A model for solar energy, *Appl. Math. Comp.*, 2014, 248, 273-286.
- [28] Das K., Acharya N., Kundu P.K., Radiative flow of MHD Jeffrey fluid past a stretching sheet with surface slip and melting heat transfer, *Alex. Eng. J.*, 2015, 54, 815-821.
- [29] Satya Narayana P.V., Harish Babu D., Numerical study of MHD heat and mass transfer of a Jeffrey fluid over a stretching sheet with chemical reaction and thermal radiation, *J. Taiwan Inst. Chem. Eng.*, 2016, 59, 18-25.
- [30] Hayat T., Bashir G., Waqas W., Alsaedi A., MHD flow of Jeffrey liquid due to a nonlinear radially stretched sheet in presence of Newtonian heating, *Results in Phy.*, 2016, 6, 817-823.
- [31] Dalir N., Dehsara M., Nourazar S.S., Entropy analysis for magnetohydrodynamic flow and heat transfer of a Jeffrey nanofluid over a stretching sheet, *Energy*, 2014, 79, 351-362.
- [32] Harish Babu D., Satya Narayana P.V., Joule heating effects on MHD mixed convection of a Jeffrey fluid over a stretching sheet with power law heat flux: A numerical study, *J. Mag. Mag. Mat.*, 2016, 412, 185-193.
- [33] Imtiaz M., Hayat T., Alsaedi A., MHD convective flow of Jeffrey fluid due to a curved stretching surface with homogeneous-heterogeneous reactions, *PLoS ONE*, 2016, 11, e0161641.
- [34] Khan M., Shahid A., Malik M.Y., Salahuddin T., Thermal and concentration diffusion in Jeffery nanofluid flow over an inclined stretching sheet: A generalized Fourier's and Fick's perspective, *J. Mol. Liq.*, 2018, 251, 7-14.
- [35] Qayyum S., Hayat T., Alsaedi A., Ahmad B., Magnetohydrodynamic (MHD) nonlinear convective flow of Jeffrey nanofluid over a nonlinear stretching surface with variable thickness and chemical reaction, *Int. J. Mech. Sci.*, 2017, 134, 306-314.
- [36] Zokri S.M., Arifin N.S., Salleh M.Z., Kasim A.R.M., Mohammad N.F., Yusoff W.N.S.W., MHD Jeffrey nanofluid past a stretching sheet with viscous dissipation effect, *J. Phys.: Conf. Series*, 2017, 890, 1-7.
- [37] Hayat T., Kiyani M.Z., Ahmad I., Khan M.I., Alsaedi A., Stagnation point flow of viscoelastic nanomaterial over a stretched surface, *Res. Phys.*, 2018, 9, 518-526.
- [38] Zhou J.K., *Differential Transformation and its Application for Electrical Circuits*, 1986, Wuhan, Huazhong University Press, China.
- [39] Hatami M., Hatami J., Jafaryar M., Differential transformation method for Newtonian and Non-Newtonian fluids flow analysis: comparison with HPM and numerical solution, *J. Braz. Soc. Mech. Sci. Eng.*, 2016, 38, 589-599.
- [40] Sobamowo M.G., Singular perturbation and differential transform methods to two-dimensional flow of nanofluid in a porous channel with expanding/contracting walls subjected to a transverse magnetic field, *Therm. Sci. Eng. Prog.*, 2017, 4, 71-84.
- [41] Usman M., Hamid M., Khan U., Mohyud Din S.T., Iqbal M.A., Wei W., Differential transform method for unsteady nanofluid flow and heat transfer, *Alex. Eng. J.*, 2018, 57, 1867-1875.
- [42] Nourifar M., Sani A.A., Keyhani A., Efficient multi-step differential transform method: Theory and its application to nonlinear oscillators, *Comm. Nonlin. Sci. Numer. Simul.*, 2017, 53, 154-183.
- [43] Shah K., Singh T., Kılıçman A., Combination of integral and projected differential transform methods for time-fractional gas dynamics equations, *Ain Shams Eng. J.*, 2018, 9, 1683-1688.
- [44] Mohamed M.S., Gepreel K.A., Reduced differential transform method for nonlinear integral member of Kadomtsev-Petviashvili hierarchy differential equations, *J. Egy. Math. Soc.*, 2017, 25, 1-7.
- [45] Abazari R., Borhanifar A., Numerical study of the solution of the Burgers and coupled Burgers equations by a differential transformation method, *Comp. Math. with Appl.*, 2010, 59, 2711-2722.
- [46] Ebaid A.E., A reliable after treatment for improving the differential transformation method and its application to nonlinear oscillators with fractional nonlinearities, *Comm. Nonlin. Sci. Num. Simul.*, 2011, 16, 528-536.
- [47] Hatami M., Sheikholeslami M., Domairry G., High accuracy analysis for motion of a spherical particle in plane Couette fluid flow by Multi-step Differential Transformation Method, *Powd. Tech.*, 2014, 260, 59-67.
- [48] Abdelghany S.M., Ewis K.M., Mahmoud A.A., Mohamed M.N., Vibration of a circular beam with variable cross sections using differential transformation method, *Beni-Suef Uni. J. Basic Appl. Sci.*, 2015, 4, 185-191.
- [49] Mirzaaghaian A., Ganji D.D., Application of differential transformation method in micropolar fluid flow and heat transfer through permeable walls, *Alex. Eng. J.*, 2016, 55, 2183-2191.
- [50] Mosayebidorcheh S., Analytical investigation of the micropolar flow through a porous channel with changing walls, *J. Molecular Liq.*, 2014, 196, 113-119.
- [51] Hatami M., Jing D., Differential Transformation Method for Newtonian and non-Newtonian nanofluids flow analysis: Compared to numerical solution, *Alex. Eng. J.*, 2016, 55, 731-739.
- [52] Rezaiee-Pajand M., Hashemian M., Modified differential transformation method for solving nonlinear dynamic problems, *Appl. Math. Mod.*, 2017, 47, 76-95.
- [53] Ganji H.F., Jouya M., Mirhosseini-Amiri S.A., Ganji D.D., Traveling wave solution by differential transformation method and reduced differential transformation method, *Alex. Eng. J.*, 2016, 55, 2985-2994.
- [54] Bozyigit B., Yesilce Y., Catal S., Free vibrations of axial-loaded beams resting on viscoelastic foundation using Adomian decomposition method and differential transformation, *Eng. Sci. Tech., Int. J.*, 2018, 21, 1181-1193.